**FIRST X-RAY DIFFRACTION RESULTS FROM MARS SCIENCE LABORATORY: MINERALOGY OF ROCKNEST AEOLIAN BEDFORM AT GALE CRATER.**

D.L. Bish[1], D.F. Blake[2], D.T. Vaniman[3], S.J. Chipera[4], P. Sarrazin[5], R.V. Morris[6], D.W. Ming[6], A.H. Treiman[7], R.T. Downs[8], C. Achilles[6], S. Morrison[8], A. Yen[9], T. Bristow[2], J. Morookian[9], J. Farmer[10], J. Crisp[9], E. Rampe[6], E. Stolper[11], D. Des Marais[2], N. Spanovich[9], R. Anderson[9] and the MSL Science Team. [1]Geol. Sci., Indiana Univ., Bloomington, IN 47405 bish@indiana.edu, [2]NASA ARC, [3]PSI, [4]CHK Energy, [5]In-Xitu, [6]NASA JSC, [7]LPI, [8]U. Arizona, [9]JPL/Caltech, [10]Arizona State U., [11]Caltech.

**Introduction:** Numerous orbital and landed observations of the martian surface suggest a reasonably uniform martian soil composition, likely as a result of global aeolian mixing [1, 2]. Chemical data for martian soils are abundant [e.g., 2, 3], and phase information has been provided by lander thermal emission and Mössbauer spectroscopic measurements [3, 4, 5, 6]. However, until now no X-ray diffraction (XRD) data were available for martian soil nor has XRD ever been used on another body apart from Earth. XRD is generally considered the most definitive method for determining the crystalline phases in solid samples, and it is the method of choice for determining mineralogy. CheMin's first XRD analysis on Mars coincided with the 100th anniversary of the discovery of X-ray diffraction by von Laue.

Curiosity delivered scooped samples of loose, unconsolidated material ("soil") acquired from an aeolian bedform at the Rocknest locality to instruments in the body of the rover (the laboratory). Imaging shows that the soil has a range of particle sizes, of 1-2 mm and smaller, presumably representing contributions from global, regional, and local sources.

**Sample and Measurement:** Scoops three, four, and five of the soil were introduced into the CHIMRA sample handling system on Curiosity. Each of these was passed through a 150 μm sieve (thus excluding the coarse-grained material visible in images of the bedform) before depositing a portion into CheMin. All materials were taken from beneath the surface layer.

Scoops three and four were placed into Kapton sample cells, and scoop five was placed into a Mylar cell. Both types of cells have the potential to contribute broad scattering signatures to the diffraction patterns. Kapton contributes a broad peak centered at ~15Å, whereas Mylar has insignificant scattering at low angles. Thus, Mylar cells are preferred when searching for diffraction signatures from phyllosilicates or other materials having diffraction peaks at low angles.

CheMin measures XRD and X-ray fluorescence (XRF) data simultaneously using Co radiation in transmission geometry. The instrument operates in single-photon counting mode so that at most one photon strikes each CCD pixel between each readout. In this way, the CCD can determine both the energy of the
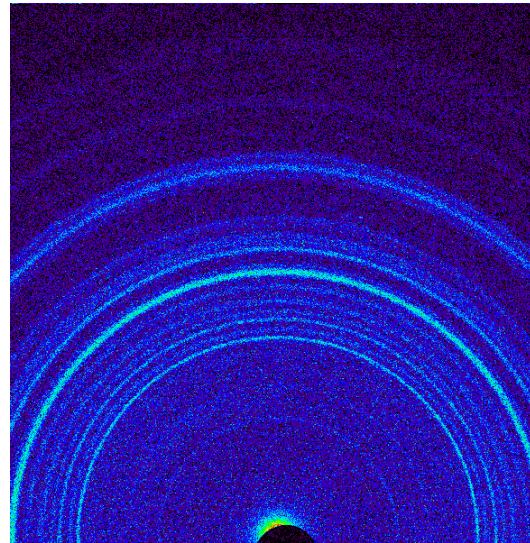


**Figure 1. 2-D XRD pattern of scoop 5; 26.9-hr integration; black semi-circle at the bottom is the beam stop.**

photons striking the CCD (XRF) and the 2-dimensional (2-D) position of each photon (XRD) [7]. The 2-D distribution of Co Kα pixels in rings represents the XRD pattern of the sample (Figure 1), and circumferential integration of these rings produces a conventional 1-D XRD pattern. This energy and positional information is summed over repeated 10-sec measurements to improve counting statistics. Each individual 10-sec measurement is generally summed into a minor frame of 30 min of data (180 frames). CheMin collects as many minor frames as possible for the available instrument time, usually five to seven per night. These are then summed to create one data file for each night of data collection. CheMin is generally operated for only a few hours each night at the lowest possible CCD temperature. Thus, XRD data were measured on several consecutive nights for each of the three scooped samples. Data were measured for 3.8 hrs (scoop 3), 15.7 hrs (scoop 4), and 26.9 hrs (scoop 5). Before analysis of each new scoop, measurements were made with the empty cell, to confirm that the cell was empty before being loaded.

**Diffraction Results:** *Crystalline components.* All XRD data were first evaluated by comparisons and searches of the ICDD Powder Diffraction File, which

revealed the presence of plagioclase feldspar, forsteritic olivine, augite, and another pyroxene. The comparatively large instrumental peak widths for the CheMin instrument limited our ability to determine accurately the presence of minor phases (<3 wt. %). These XRD data were analyzed further via Rietveld methods, using the Bruker AXS Topas package. Rietveld refinements using numerous potential possibilities revealed the likely presence of pigeonite with augite. Refinements using augite with orthopyroxene or clinopyroxene were inferior to an augite-pigeonite model. A single plagioclase model was as good as a model with two plagioclases. Refinements also clarified the minor phases and allowed exclusion of many possibilities. The presence of minor phases was evaluated individually by including each in the model and evaluating their effect on the fit. Using this approach, we found no evidence for the presence of any perchlorate, carbonate, sulfate (apart from anhydrite), or phyllosilicate. Refinement results for scoop five are shown in Figure 2, and the mineralogy is given in Table 1 (normalized to 100% crystalline components). All three scoop samples produced similar results. The 2σ values given in Table 1 are taken from the Rietveld refinement output and are considered optimistic; they show that several minor phases are questionable, where errors are close to or exceed the stated value. Rietveld refinement also provides unit-cell parameters for all phases, and compositional information was estimated from these values [8].

*Amorphous or poorly ordered components.* The background curve inscribed beneath the profiles in Figure 2 emphasizes the elevated background in the 15-40º 2θ range, due to the presence of one or more amorphous or poorly ordered components. The low-angle background is also elevated significantly above that seen with empty cells. XRD data were thus also analyzed using the FULLPAT program [9], which gave 27% amorphous content. We used a synthetic Gusev-
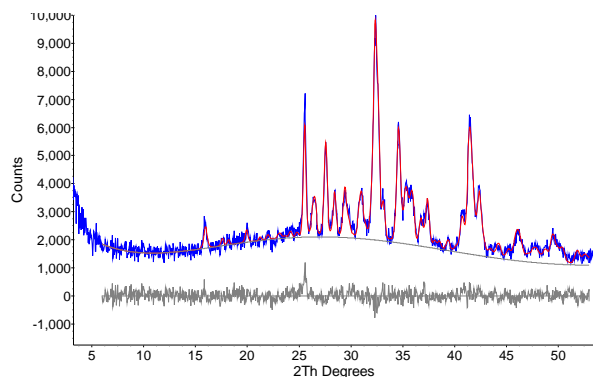
**Table 1. Crystalline components (amorphous-free) of the Rocknest scoop 5 soil.**

| Mineral | Wt.% | 2σ |
|---|---|---|
| Andesine (~An50) | 42.9% | 3.4% |
| Forsterite (~Fo58) | 20.5% | 2.6% |
| Augite | 16.7% | 3.5% |
| Pigeonite | 11.4% | 3.9% |
| Sanidine | 2.1% | 1.9% |
| Magnetite | 1.8% | 1.1% |
| Quartz | 1.7% | 0.7% |
| Anhydrite | 1.4% | 0.9% |
| Hematite | 0.8% | 1.1% |
| Ilmenite | 0.7% | 1.2% |

composition basaltic glass as one of our standards, but the exact nature of the amorphous component remains unclear, and SAM and MER Mössbauer data support the presence of a hydrated amorphous phase containing $Fe^{3+}$. The uncertainty on this value may be as high as 50% relative. The sample also may contain a small amount of material resembling allophane or hisingerite, based on the elevated low-angle background.

**Summary:** These first XRD data from another planet reveal a rich mineralogic inventory in these scooped samples, showing that the mineralogy is remarkably similar to that found on Earth in places such as soils on the flanks of Mauna Kea volcano, Hawaii. It is also noteworthy that the crystalline component is very similar to normative basalt mineralogies predicted from Gusev [10] and is also qualitatively similar to mineralogies of martian basaltic meteorites. Thus the results may be applicable to previous and future soil measurements on Mars, as soil compositions from many different measurements appear so similar. By combining these XRD results with compositional estimates from unit-cell parameters and bulk chemistry, it will be possible to make determinations of individual phase compositions, including that of the amorphous components [11]. Thus these data will provide valuable ground truth information on martian soils.

**References:** [1] Clark B. C. et al. (1982) *JGR, 87,* 10059-10067. [2] Gellert R. et al. (2004) *Science, 305,* 829-832. [3] Yen A. S. et al. (2005) *Nature 436,* 49-54. [4] Morris R. V. et al. (2006) *JGR, 111,* E12S15. [5] Morris R. V. et al. (2004) *Science, 205*, 833-836. [6] Christensen P. R. et al. (2004) Science, *306*, 1733-1739. [7] Blake D. F. et al. (2012) *Space Sci. Rev.* doi: 10.1007/s11214-012-9905-1. [8] Morrison S. M. et al. (2013) *LPS XLIV,* Abstract. [9] Chipera S. J. and Bish D. L. (2002) *J. Appl. Cryst., 35*, 744-749. [10] Ming D. W. et al. (2008) *JGR, 113,* E12S39. [11] Morris et al. (2013) *LPS XLIV,* Abstract.



**Figure 2. Rietveld refinement results for scoop 5. Observed (blue) versus calculated (red) pattern, with difference curve at the bottom.**